Hindawi Publishing Corporation
Mathematical Problems in Engineering
Volume 2014, Article ID 743904, 12 pages
http://dx.doi.org/10.1155/2014/743904

Research Article

Optimal Sensor Placement for Latticed Shell Structure Based on an Improved Particle Swarm Optimization Algorithm

Xun Zhang,[1] Juelong Li,[2] Jianchun Xing,[1] Ping Wang,[1] Qiliang Yang,[1] Ronghao Wang,[1] and Can He[1]

[1] *College of Defense Engineering, PLA University of Science and Technology, Nanjing 21007, China*
[2] *Technical Management Office of Naval Defense Engineering, Beijing 100841, China*

Correspondence should be addressed to Xun Zhang; xunzhang893@163.com

Received 19 February 2014; Revised 22 May 2014; Accepted 22 May 2014; Published 16 June 2014

Academic Editor: Fang Zong

Optimal sensor placement is a key issue in the structural health monitoring of large-scale structures. However, some aspects in existing approaches require improvement, such as the empirical and unreliable selection of mode and sensor numbers and time-consuming computation. A novel improved particle swarm optimization (IPSO) algorithm is proposed to address these problems. The approach firstly employs the cumulative effective modal mass participation ratio to select mode number. Three strategies are then adopted to improve the PSO algorithm. Finally, the IPSO algorithm is utilized to determine the optimal sensors number and configurations. A case study of a latticed shell model is implemented to verify the feasibility of the proposed algorithm and four different PSO algorithms. The effective independence method is also taken as a contrast experiment. The comparison results show that the optimal placement schemes obtained by the PSO algorithms are valid, and the proposed IPSO algorithm has better enhancement in convergence speed and precision.

1. Introduction

Many large-scale civil infrastructures have been established with the rapid development of engineering technology. However, these structures are easily damaged in their long service lives because of inadequate designs and increasing traffic loads, which may cause sudden destruction and large economic losses. Therefore, developing a continuous structural health monitoring (SHM) system is essential. The sensor system is an important subsystem of a typical SHM system. More information can generally be obtained with the increasing sensor number. Unfortunately, an excessive sensor number increases the testing cost, which also increases the SHM system cost. Installing sensors are also difficult in many parts of the structure. Thus, designing an optimal sensor scheme is a key issue. The optimal placement of sensors not only lowers the cost but also acquires reliable and comprehensive structural health information [1]. Therefore, how to determine the optimal number of sensors and where to arrange the limited sensors have become key research issues.

Over the past two decades, large quantities of optimal sensor placement (OSP) techniques and criteria have been proposed for modal parameter identification and health monitoring of structures. These techniques can be divided into two categories, namely, traditional iterative approaches and global optimization techniques. The information-theory-based approaches are the important parts of the traditional iterative approaches. Kammer [2], Udwadia [3], Kammer and Tinker [4], and Meo and Zumpano [5] have all proposed information-theory-based approaches to select the optimal sensor locations. In these methods, the optimal sensor set is selected by maximizing the determinant of the Fisher information matrix. Papadimitriou [6, 7] used the information entry as a criterion to determine the optimal sensor configuration. Trendafilova et al. [8] addressed the concept of average mutual information to identify the optimal sensor locations. The matrix-decomposition-based approaches are also applied to OSP. Schedlinski and Link [9] introduced QR-decomposition of the modal matrix to determine the optimal sensor locations. Park and Kim [10], Cherng [11], and Reynier

and Abou-Kandil [12] have all adopted singular value decomposition methods to place sensors at optimal locations. Other iterative methods, such as the Guyan reduction [13], modal kinetic energy [14, 15], eigenvector component product [16], and drive point residue [17], have also been presented to solve the OSP problem. In recent years, with the rapid development of computational intelligence approaches, some global optimization techniques such as genetic algorithms (GAs) [18–24] and particle swarm optimization (PSO) algorithms [25–27] have been employed to determine the OSP. Given their advantages over traditional iterative methods such as global search, efficient parallel, and robustness, global optimization algorithms have played an important role in solving the OSP problem.

The above approaches could be applied to solve practical OSP problems and have already made great progress. However, some defects still exist in these methods. Firstly, the basic data selection for OSP is empirical. Generally, the mode shape matrix attained through modal analysis is always used for solving the OSP problem. Considering that the mode shape matrix is composed of modes, different mode shape matrices can be obtained with different mode numbers. This scenario leads to different sensor placement results. Therefore, how to select the modes is very important. In the previous methods, the lower modes were considered to have larger contributions to the dynamic response and always selected based on experience for solving the OSP problem. This mode selection method is unreasonable to a certain extent. Secondly, determining the optimal sensor number for specific structural forms is difficult. In general, the sensor number is predefined to a desired one or is determined based on the relationship between the fitness value and different sensor numbers. However, the predefined sensor number is subjective. The fitness value used for determining the sensor number is also computed only once. This condition will result in unreliable and imprecise computation results. Finally, the effective performance of the optimal placement techniques may not be assured. In traditional approaches, the computation of the desired sensor locations is an iterative process that usually obtains the suboptimal rather than the optimal value. Thus, this condition expands the errors between the real and estimated modal parameters identified by the placed sensors of these techniques. For the global optimization techniques, some features of the GA-based algorithms still require improvement. For example, it takes more computation time for the GAs to search for the best sensor locations because of the computational complexity. In view of this, Yao et al. [18] lowered the number of possible candidate sensor locations before applying GA to limit the complexity. Rao and Anandakumar [25] claimed that the GA performance for the OSP is difficult to assure if the problems have large candidate sensor configurations. Thus, they proposed a hybrid swarm intelligence technique to solve the OSP problem without limiting the number of possible candidate sensor configurations. Lian et al. [26] also used a hybrid swarm intelligence algorithm for OSP. The optimized results show that the proposed algorithm outperforms a GA in the capability of global optimization.

Concerning the existing problems and advantages of the swarm intelligence algorithm over GA, this paper proposes a type of improved particle swarm optimization (IPSO) algorithm to solve the OSP problem better. The cumulative effective modal mass participation ratio is firstly proposed to select the reasonable number of modes. Three strategies are then used to improve the PSO algorithm, including the dual-structure coding, novel inertia weight adjustment method, and mutation operator. The root mean square value of the off-diagonal elements in the modal assurance criterion (MAC) matrix is also taken as the fitness function. Finally, the IPSO algorithm is employed to solve the OSP problem of a latticed shell structure. The simulation experiments compared with the effective independence (EI) method and four different PSO algorithms variants are also conducted to verify the performance of the proposed algorithm.

The remaining part of this paper is organized as follows. Section 2 introduces the background of the OSP problem. Section 3 presents the OSP implementation steps based on the proposed IPSO algorithm. Section 4 shows the performance of the proposed IPSO algorithm for optimizing OSP in a latticed shell structure. Section 5 is some conclusions and the future work.

2. Background

Placing sensors at every degree of freedom (DOF) for structures is impossible because of the high cost of sensors, data acquisition system, and data processing system. The goal of OSP is to acquire the maximum structural health information by placing as few sensors as possible and make sure that the sensor locations are the best. Suppose the number of nodes in a structure is m, the numbered nodes compose a set N, where $N = \{n_1, n_2, \ldots, n_m\}$, the theoretical DOF of n_i is x_i $(i = 1, 2, \ldots, m)$, and the DOFs of all nodes compose a set $X = \{x_1, x_2, \ldots, x_m\}$. Given the constraints of the installation process, x_1, x_2, …, x_s $(s \leq m)$ of the set X are selected as the candidate sensor locations. The goal is to search for the optimal ones from the candidates. Thus, OSP can be presented as an optimal problem that consists of the objective function and constraints as follows:

$$\begin{aligned} &\min \quad f(x) \\ &\text{s.t.} \quad x = (x_1, x_2, \cdots, x_s) \subset X, \end{aligned} \tag{1}$$

where $f(x)$ is the objective function with the decision variables, $x_1, x_2, \ldots, x_s$. This condition is a minimum optimization problem. The key is to find the minimum value of f with respect to the decision variables, where x_j $(x_j \in x)$ is one of them. If $x_j = 1$, then a sensor is placed at the j-th DOF; if $x_j = 0$, no sensor exists. Once x_j is confirmed, the locations of the sensors can thus be determined.

The PSO algorithm is a swarm intelligent computation technique based on a simple simulation of bird flocking, fish schooling, and swarming theory. Unlike other evolutionary computation techniques, the PSO algorithm is simple, easy to implement, and computationally efficient. This algorithm has attracted much attention since its first introduction in 1995 [28, 29]. The PSO algorithm also has science and engineering applications. In PSO, each solution point in the search space is

known as a particle. The particle can find the optimal position through its own experience and social cooperation with its neighbors. All particles are assigned a random velocity. The particles fly through the problem space with a certain velocity to reach better search areas. Suppose each particle searches for the optimal value in the D-dimensional problem space, $X_i = (X_{i1}, X_{i2}, \ldots, X_{iD})$ is the position of the ith particle, $V_i = (V_{i1}, V_{i2}, \ldots, V_{iD})$ represents the velocity of the particle, which is clamped to a maximum magnitude "$V_{\max}$" specified by the problem to be solved, $P_i = (P_{i1}, P_{i2}, \ldots, P_{iD})$ is the best previous position for the ith particle, and $P_g = (P_{g1}, P_{g2}, \ldots, P_{gD})$ is the best previous position of the swarm. The velocity V_{id} and position X_{id} update equations are given as follows:

$$V_{id}^{t+1} = V_{id}^{t} + c_1 r_{1id}\left(P_{id} - X_{id}^{t}\right) + c_2 r_{2id}\left(P_{gd} - X_{id}^{t}\right)$$
$$X_{id}^{t+1} = X_{id}^{t} + V_{id}^{t+1}, \tag{2}$$

where c_1 and c_2 are the acceleration coefficients, which are normally taken as 2, t is the current iteration number, d is the current dimensional problem space, and r_1 and r_2 are independently uniformly distributed random numbers in the range of $[0, 1]$.

3. Proposed IPSO Algorithm for OSP

In this section, a new approach called IPSO algorithm is proposed to solve the existing sensor placement problems in traditional methods. Three steps are included in this approach, which can be seen in Figure 1. The mode number is initially selected based on the cumulative effective modal mass participation ratio. A novel IPSO algorithm is also proposed based on three different strategies. Finally, this proposed IPSO algorithm is applied to determine the optimal sensor number and configurations.

3.1. Mode Selection. Modal analysis can provide the original data for OSP (i.e., mode shape matrix), which is composed of modes. How to select mode number is very important. If the number is different, the same optimization algorithm obtains different location schemes. The computation is also time-consuming given an excessive number of modes. Thus, selecting proper modes before using the placement method to determine the sensor locations is essential. In this section, the effective modal mass participation ratio is employed to determine the main modes, and the cumulative effective modal mass participation ratio is adopted to decide the proper mode number. The computational method on the selection of modes is studied using the following mathematical derivation.

The basic motion equation of a general n-DOF system subjected to an external force can be described as follows:

$$M\ddot{u} + C\dot{u} + Ku = -Me\ddot{u}_a(t), \tag{3}$$

where n is the number of DOFs; M is the mass matrix; C is the damping matrix; K is the stiffness matrix; e is the direction matrix of the external force; $\ddot{u}_a(t)$ is the acceleration impact

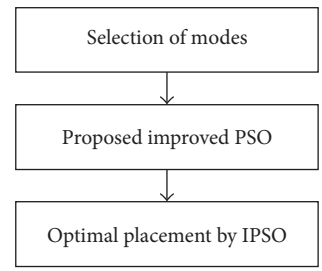

Figure 1: Steps of the IPSO method for OSP.

generated by the external force; and $\ddot{u}$, $\dot{u}$, and u are the acceleration, velocity, and displacement response, respectively.

Using the mode shape matrix Φ to express the structural response, the following values are obtained:

$$u = \Phi q, \qquad \dot{u} = \Phi\dot{q}, \qquad \ddot{u} = \Phi\ddot{q}. \tag{4}$$

Considering the orthogonal conditions of M, C, and K, as well as combining (3) and (4), we can obtain the following:

$$\ddot{q}_i + 2\zeta_i w_i \dot{q}_i + w_i^2 q_i = -\frac{\phi_i^T Me}{\phi_i^T M\phi_i}\ddot{u}_a(t), \tag{5}$$

where q_i is the modal coordinate, w_i is the natural frequency, ζ_i is the modal damping ratio associated with the ith mode, and ϕ_i is the ith column vector in the matrix Φ.

The modal participation factor can be defined as follows:

$$\gamma_i = \frac{\phi_i^T Me}{\phi_i^T M\phi_i}. \tag{6}$$

Normalizing the modal mass by the following equation:

$$\phi_i^T M\phi_i = 1, \tag{7}$$

the modal participation factor can be expressed as follows:

$$\gamma_i = \phi_i^T Me. \tag{8}$$

We define the effective modal mass of the ith mode as follows:

$$M_i = \frac{\gamma_i^2}{\phi_i^T M\phi_i}. \tag{9}$$

Considering (7), we can obtain $M_i = \gamma_i^2$, and the total mass can be derived from the following:

$$\sum_{i=1}^{n} M_i = \sum_{i=1}^{n} \gamma_i^2 = \gamma^T\gamma. \tag{10}$$

From (8), we can obtain $\gamma = \Phi^T Me$. Substituting this equation into (10), we can reach the following equation:

$$\gamma^T\gamma = \left(\Phi^T Me\right)^T\left(\Phi^T Me\right) = \left(e^T M\Phi\right)\left(\Phi^T Me\right). \tag{11}$$

The matrix form of (7) can be expressed as follows:

$$I = \Phi^T M\Phi = \left(\Phi^T M\Phi\right)^{-1}, \tag{12}$$

where I is a unit matrix. Substituting (12) into (11), we can obtain the following:

$$\begin{aligned}\gamma^T\gamma &= \left(e^T M\Phi\right)\left(\Phi^T Me\right)\\ &= \left(e^T M\Phi\right)\left(\Phi^T M\Phi\right)^{-1}\left(\Phi^T Me\right)\\ &= e^T M\Phi\Phi^{-1}\left(\Phi^T M\right)^{-1}\left(\Phi^T M\right)e\\ &= e^T Me\\ &= m_1 + m_2 + \cdots + m_n\\ &= M_T.\end{aligned} \tag{13}$$

The above equation indicates that the total effective modal mass is equal to the total mass or the rotational inertia. Thus, the ith effective modal mass is one of the important parameters that can reflect the dynamic response of the given modes. It can be used to determine the mode number.

We define the ratio of effective modal mass to total effective modal mass as the effective modal mass participation ratio. The effective modal mass participation ratio with respect to the ith mode can be presented as follows:

$$r_i = \frac{M_i}{e^T Me}. \tag{14}$$

In practical calculation, if the number of modes is k ($k < n$), then the cumulative effective modal mass participation ratio can be expressed as follows:

$$R = \sum_{i=1}^{k} r_i. \tag{15}$$

The above equation reflects the effective modal mass participation ratio of the selected modes. The R value should be larger than 90% (i.e., $R \geq 0.9$) to obtain a sufficient number of main modes [30]. This criterion is applied to select the mode number.

3.2. OSP Using the IPSO Algorithm. The proposed novel IPSO algorithm is designed to solve the OSP problem. The flow chart of the designed algorithm is presented in Figure 2. Firstly, the population is initialized and the values of P_i and P_g are calculated. The parameters are updated, and the fitness values are evaluated. The mutation operator is employed if the fitness value does not improve over the iterations; P_i and P_g are updated otherwise. Finally, the second step is repeated until the termination condition is satisfied.

3.2.1. Initialization. Initializing position and velocity of the particle are two basic aspects. As the goal of the algorithm is to determine the optimal fitness value with respect to the particle's position, the position initialization directly determines the search result. Thus, the computation performance of the algorithm is greatly affected by the position. The initialization of the particle's position is thus mainly introduced as follows. However, the velocity is randomly initialized in the search space.

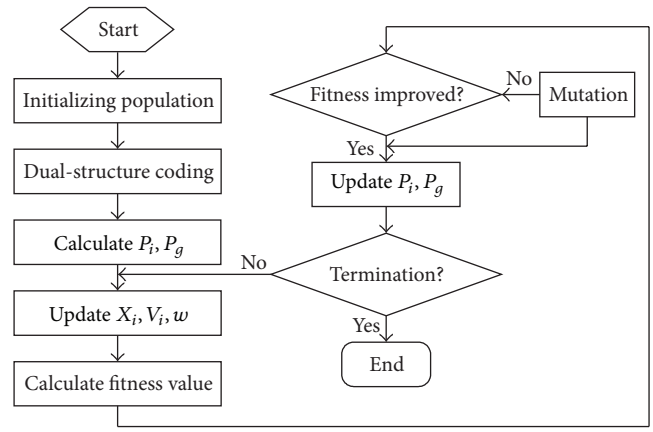

Figure 2: Flow chart of the proposed IPSO algorithm.

Table 1: A new particle position generated by dual-structure coding method.

Extra code	$P(1)$	$P(2)$	$\cdots$	$P(i)$	$\cdots$	$P(s)$
Variable code	$K_{P(1)}$	$K_{P(2)}$	$\cdots$	$K_{P(i)}$	$\cdots$	$K_{P(s)}$

Table 2: Example of a dual-structure coding method.

2	3	1	5	7	4	10	6	9	8
0	1	1	0	0	0	1	0	1	1

The position initialization is assumed to be a coding problem. The 1D binary coding method can be used to initialize the particle's position. The length of the binary string should be the same as the candidate sensor locations. If the value of the ith code is 1, a sensor is placed on the ith DOF. Otherwise, no sensor exists. This coding method is simple, intuitional, and easy to implement. However, the sensor number changes if 1 is changed in the particle's position code. Thus, this coding method is improper for solving the OSP problem. A dual-structure coding method is adopted in [31]. This method can overcome the shortcomings of binary coding. The dual-structure coding method is thus employed in the particles' position encoding of the PSO algorithm. The specific method can be described as follows.

The upper line is the extra code, which is generated randomly through the shuffle method firstly. The variable code is then produced randomly (with a value of 0 or 1) and placed on the lower line. Thus, the extra and variable codes compose the individual position. A particle's position encoded by the dual-structure method can be seen in Table 1. The upper line $P(i)$ is the extra code of K_j, where $P(i) = j$ and the length of extra code is equal to the length of the candidate sensor locations (i.e., s in this paper). The lower line denotes the variable code $K_{P(i)}$ corresponding to the extra code $P(i)$. When decoding the variable code, the constraints should be considered, and the penalty function is used. If a variable does not follow the constraints, its corresponding value is enforced to be 0 or 1 if otherwise.

For example, an OSP problem with 10 candidate sensor locations and the randomly generated sequence of extra code

is (2, 3, 1, 5, 7, 4, 10, 6, 9, and 8). Its dual-structure code is presented in Table 2. In this manner, the code corresponds to a feasible solution (i.e., the 1st, 3rd, 8th, 9th, and 10th DOFs are selected as the sensor locations).

3.2.2. Improved Inertia Weight Adjustment Strategy. The PSO algorithm shows significant performance in the initial iterations, but it might encounter local optimum in the latter iterations. Many researchers have worked on improving its performance by dynamically changing the PSO parameters during the iterations. Shi and Eberhart [32] introduced an inertia weight w into the original PSO algorithm to improve its performance. This parameter can provide a flexible influence of the previous velocity on the new velocity. This modified PSO algorithm is a standard PSO (SPSO). The velocity updating of the d-th dimension of the ith particle in the SPSO algorithm is presented as follows:

$$V_{id}^{t+1} = wV_{id}^{t} + c_1 r_{1id}\left(P_{id} - X_{id}^{t}\right) + c_2 r_{2id}\left(P_{gd} - X_{id}^{t}\right). \quad (16)$$

The inertia weight w reflects the particle's dynamic behavior. A higher value is good for globally exploring a better solution. However, a lower inertia weight could provide slower updating in exploring locally. A linear inertia weight adjustment strategy is proposed in [33] to balance the global and local search capabilities. Thus,

$$w(t) = w_{\max} - \left(w_{\max} - w_{\min}\right)\frac{t}{t_{\max}}, \quad (17)$$

where $w_{\max}$ is the maximum value of the w, $w_{\min}$ is the minimum value of the w, $t_{\max}$ is the maximum number of allowable iterations, and t is the current number of iterations. Shi and Eberhart [33] conducted empirical studies and found that the optimal value can be improved when the value of w is linearly decreased in the range of [0.9, 0.4]. This PSO is thus referred to as linearly decreasing inertia weight PSO (LPSO).

Eberhart and Shi [34] applied PSO algorithm to track and optimize dynamic systems. However, they found that the improved LPSO algorithm is not very effective in tracking dynamic systems. Instead, they took the dynamic nature of real-world application into consideration and proposed a random inertia weight factor for tacking dynamic systems. The difference between this method and LPSO is that the inertia weight w changes randomly as follows:

$$w(t) = 0.5 + \frac{r_3}{2}, \quad (18)$$

where r_3 is the same as r_1 or r_2 (i.e., it is a random number in the range of $[0, 1]$). For the remainder of this paper, this PSO algorithm is referred to as random inertia weight PSO (RPSO).

A nonlinear time-varying inertia weight strategy was proposed in [35]. The inertia weight nonlinearly decreased from a high initial value $w_{\max}$ to $w_{\min}$. The main difference between this method and LPSO is the following inertia weight decreasing strategy:

$$w(t) = w_{\min} + \left(\frac{t_{\max} - t}{t_{\max}}\right)^{\alpha}\left(w_{\max} - w_{\min}\right), \quad (19)$$

where $w_{\max}$ is the maximum value of the w, $w_{\min}$ is the minimum value of the w, $t_{\max}$ is the maximum number of allowable iterations, t is the current number of iterations, and α is the nonlinear modulation exponent. The proper choice of exponent α is one of the important factors in successfully implementing this algorithm. $\alpha = 1.2$ has shown encouraging results from several benchmark simulations. This algorithm with $\alpha = 1.2$ is referred to as nonlinearly decreasing inertia weight PSO (NPSO).

Given the results in [35], we developed a PSO algorithm based on the nonlinearly decreasing inertia weight strategy. However, unlike the NPSO method in [35], the proposed inertia weight nonlinearly decreases from $w_{\max}$ to $w_{\min}$ based on the cosine function feature. The nonlinear inertia weight strategy can be mathematically presented as follows:

$$w(t) = w_{\min} + \left(\frac{1 + \cos\left(t\pi/t_{\max}\right)}{2}\right)^{k}\left(w_{\max} - w_{\min}\right), \quad (20)$$

where $w_{\max}$ is the maximum value of the w, $w_{\min}$ is the minimum value of the w, $t_{\max}$ is the maximum number of allowable iterations, t is the current number of iterations, and k is a positive constant, which can adjust the slope of the decreasing curve of the inertia weight. The decreasing curves with different k value can be seen in Figure 3.

The k value is important in determining the decreasing pattern of the inertia weight. When k is less than 1.0, the inertia weight decreases according to the convex function; when k is larger than 1.0, the inertia weight strategy is based on the convex and concave strategies. The inertia weight value is higher in the early iterations and quickly decreases during the latter iterations compared with the linearly decreasing strategy. The major consideration of this improvement is avoiding premature convergence in the early part of the search and enhancing convergence to the global optimum in the latter part. As mentioned above, a higher inertia weight in the early stages and a lower inertia weight during the latter stages can meet this demand. Through many simulation experiments, the algorithm shows better convergence performance with the increasing k value. We only considered the proposed nonlinearly decreasing strategy with $k = 10$ to take advantage of this proposed strategy and simplify this problem. In the remainder of this paper, this proposed PSO algorithm is referred to as the improved PSO (IPSO).

3.2.3. Mutation Operator. The fast decreasing inertia weight during the latter optimization stages can enhance the convergence rate. However, this condition may result in the lack of population diversity and may rush to a local optimum solution. Attempts have been made in the literature to devise the behavior of the particles in the latter range of the search space and improve the population diversity. Therefore, the concept of "mutation" has been observed to enhance the PSO algorithm performance in [36].

According to this new strategy, a particle is firstly picked randomly, and then a random perturbation is added to the velocity of that selected particle by a predefined mutation probability. In this study, the mutation operator is obtained using the strategy proposed in [36], which set the random

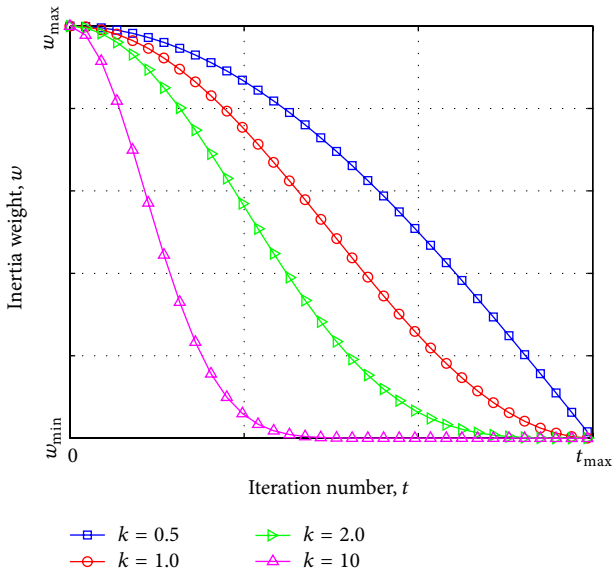

Figure 3: The cures of inertia weight with different value of k.

```
if (Δglobal ≤ 0)
  if (rand1(·) < Pm)
    if (rand2(·) < 0.5)
      vkl = vkl + rand3(·) ∗ Vmax/m;
    else
      vkl = vkl − rand4(·) ∗ Vmax/m;
    end if
  end if
end if
```

Algorithm 1

perturbation proportional to the maximum allowable velocity. The chief pseudocode for the mutation strategy is as in Algorithm 1, where Δglobal is the divergence of the global solution over the adjacent two generations, $\text{rand}_i(\cdot)$, $i = 1, 2, \ldots, 4$, are independently uniformly distributed random numbers in the range of $[0, 1]$, P_m is the mutation probability, k and l are random constants, and m is a constant, which can control the mutation step size.

Through numerical simulations, the parameters setting of the PSO algorithm with the mutation strategy are supplied in [36]. In this investigation, the same parameter setting is used. In particular, P_m is set to 0.4, and the mutation step size is set to linearly decrease from V_{max} to $0.1V_{max}$ during the search space.

3.2.4. Fitness Function. The quality of the new individuals is judged by the fitness function value in the optimization algorithm. For the PSO algorithm, the fitness value in the search space is used to evaluate the solution directly. Thus, the fitness function is very important for the PSO algorithm and should be selected properly.

The measured mode shape vectors should be linearly independent as much as possible to distinguish the measured modes. Carne and Dohrmann [37] pointed that the MAC is a good tool to evaluate this linear dependence. The MAC value compares the direction of the two vectors. When the MAC value is relatively small, the two vectors are easily distinguishable. Thus, the off-diagonal terms of the MAC matrix can be used to check the linear independence of the mode shapes. The MAC matrix elements can be expressed as follows:

$$\text{MAC}_{ij} = \frac{\left(\phi_i^T \phi_j\right)^2}{\left(\phi_i^T \phi_i\right)\left(\phi_j^T \phi_j\right)}, \tag{21}$$

where ϕ_i and ϕ_j are the mode shape vectors for the ith and j-th modes.

The root-mean-square (RMS) value reflects the magnitude and size of a data group. Therefore, the RMS value of the whole off-diagonal elements in the MAC matrix can be utilized to construct the fitness function. The equation of the optimization objective function [38] can be presented as follows:

$$f = \sqrt{\frac{1}{n(n-1)} \sum_{i=1}^{n} \sum_{j=1}^{n} \text{MAC}_{ij}^2}, \quad (i \neq j), \tag{22}$$

where n is the MAC matrix dimension. Thus, the function indicates the change in the off-diagonal elements in the MAC matrix, and the value should be as small as possible.

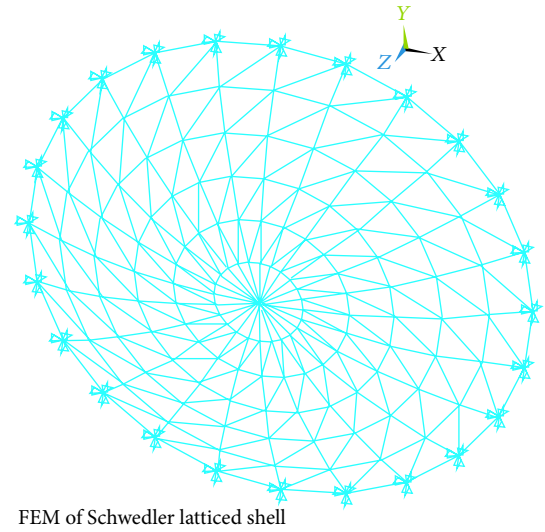

Figure 4: Finite element model of the latticed shell.

4. Sensor Placement Simulation

In this section, a numerical experiment is conducted to test and validate the proposed IPSO algorithm for the OSP problem. The EI method and five other PSO algorithms in Section 3.2.2 are also used for comparison.

4.1. Modeling and Modal Analysis. The considered numerical example is a single layer Schwedler latticed shell. The total span of the latticed shell is 100 m and the rise is 6.7 m. The

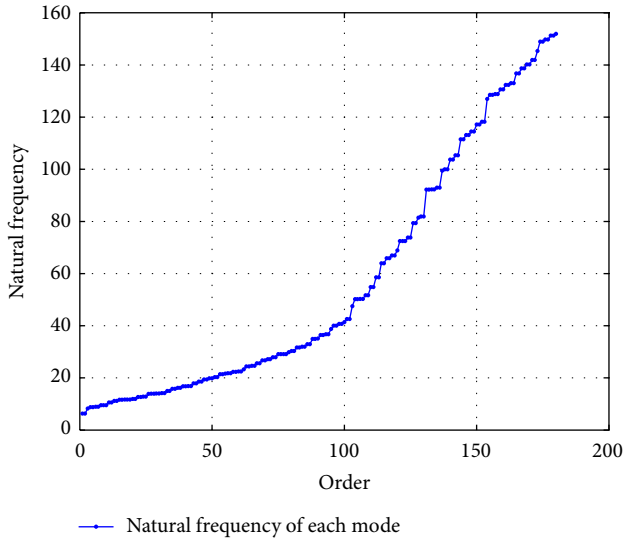

Figure 5: Natural frequency with respect to each mode.

grid numbers in the circumferential and radial directions are 24 and 6, respectively. All elements are tubular, and the specifications are Ø92.5 mm × 2.5 mm and Ø83 mm × 3 mm. The material properties are obtained from Q235 steel, the elastic modulus of the material is 210 GPa, and the mass density is 7850 kg/m^3. The shell is clamped on a fixed-point at the rim of the shell. The total element, node, and candidate DOF numbers are 408, 145, and 363, respectively. The finite element model (FEM) of the Schwedler latticed shell is created using the finite element analysis package (ANSYS [39]) to obtain the mode shape matrix. The obtained FEM of the latticed shell is shown in Figure 4. The structural dynamic characteristics, including the natural frequencies and normalized mode shapes, are also calculated by performing modal analysis based on the subspace iteration method. The natural frequency with respect to each order mode is shown in Figure 5. The first seven mode shapes and corresponding frequencies are shown in Figure 6.

4.2. Mode Number. In Figures 5 and 6, the distribution of the natural frequencies is very dense, and the mode shapes are complicated in the lower order modes. Some higher modes also have larger contributions to the vibration response of structure with different environmental incentives [40]. Therefore, selecting the main modes is essential. In this study, the cumulative effective modal mass participation ratio is used to determine the main contribution modes. As mentioned above, every effective modal mass participation ratio should be calculated until the cumulative effective modal mass participation ratio is larger than 90%. The main modes are then selected according to the larger ones. The selected main modes, effective modal mass, effective modal mass participation ratio, and cumulative effective modal mass participation ratio in the three directions (i.e., x, y, and z directions) are listed in Table 3.

As shown in Table 3, the 1st, 6th, 18th, and 80th modes are selected in the x direction; the 2nd, 7th, 17th, and 81st modes are selected in the y direction; and the 3rd, 8th, 19th, and 26th modes are selected in the z direction. The cumulative effective modal mass participation ratios of the three directions are R_x = 93.48%, R_y = 93.48%, and R_z = 91.38%, respectively, which are larger than the criterion at 90%. Thus, we considered that the selected mode number includes sufficient main modes.

4.3. Sensor Number. The sensor number is one of the key issues in OSP problems. In this section, the proposed IPSO algorithm is introduced to search for the best fitness value with respect to each sensor number. A circulating computation strategy is adopted to determine the optimal sensor number and enhance the precision and reliability of the computation result. With this strategy, the mean best fitness can be obtained. The sensor number is μ, and the mean best fitness value is f. Thus, the μ-f curve can be obtained, which indicates the relationship between the sensor number and the mean best fitness value. In this curve, the stable point demonstrates that the fitness does not change or only slightly changes with the increase in the sensor number. Therefore, the corresponding sensor number of this point is the economical one. This computation method's flow chart is shown in Figure 7.

For each computation, this method calculates the fitness value of each sensor. For each sensor, the IPSO algorithm repeats the maximum number of allowable iterations to search for the best fitness value. Therefore, this approach becomes complex and time-consuming if the maximum computation trial, sensor number, and allowable iterations are too large. We are also more concerned about the stable point of the μ-f curve than the calculating accuracy for the given problem. The maximum computation trial is set to 10, the maximum sensor number is set to 30, and the maximum number of allowable iterations is set to 100 so as to lower the computation complexity. The mutation probability P_m = 0.4, and mutation step size linearly decreases in the range of [$V_{\max}$, $0.1V_{\max}$]. The acceleration coefficients $c_1 = c_2 = 2.0$, the population size $N = 40$, and the maximum velocity $V_{\max}$ is equal to the candidate DOFs (i.e., $V_{\max} = 363$). The obtained μ-f curve for the 10 trials can be seen in Figure 8. The mean best fitness value clearly becomes smaller with the increase in the sensor number. This condition indicates that more information can be obtained with more sensors placed on the structures. The decreasing rate of the mean best fitness value becomes slow when the number of sensors increases to 20. Thus, we considered 20 as the stable point of the μ-f curve and set the economical sensor number to 20.

4.4. Results of the Contrast Experiments and Analysis. The comparison simulations of EI, SPSO, LPSO, NPSO, and RPSO algorithms are conducted to assess the proposed IPSO algorithm's performance. The inertia weight adjustment strategies of the five different PSO algorithms are set as follows. In SPSO, the inertia weight is fixed at 0.9. In LSPO, the inertia weight linearly decreases from 0.9 to 0.4. In NPSO, the inertia weight nonlinearly decreases from 0.2 to −0.3 with the slope $m = -2.5 \times 10^{-4}$ and exponent $\alpha = 1.2$. In RPSO, the inertia weight changes randomly according to (18). In the proposed IPSO, the inertia weight nonlinearly decreases from 0.9 to 0.4 with the exponent $k = 10$ as described

Table 3: The selected main modes, effective modal mass (EM), effective modal mass participation ratio (EPMR), and cumulative effective modal mass participation ratio (CEMR) in the three directions.

	x direction			y direction				z direction			
Order	EM	EPMR	CEMR	Order	EM	EMPR	CEMR	Order	EM	EMPR	CEMR
1	1569.2	10.15%	10.15%	2	1569.2	10.15%	10.15%	3	1983.6	11.55%	11.55%
6	2043.4	13.22%	23.37%	7	2043.4	13.22%	23.37%	8	2800.4	16.31%	27.86%
18	781.19	5.05%	28.42%	17	781.21	5.05%	28.42%	19	10550	61.45%	89.31%
80	10056	65.06%	93.48%	81	10056	65.06%	93.48%	26	433.34	2.52%	91.83%

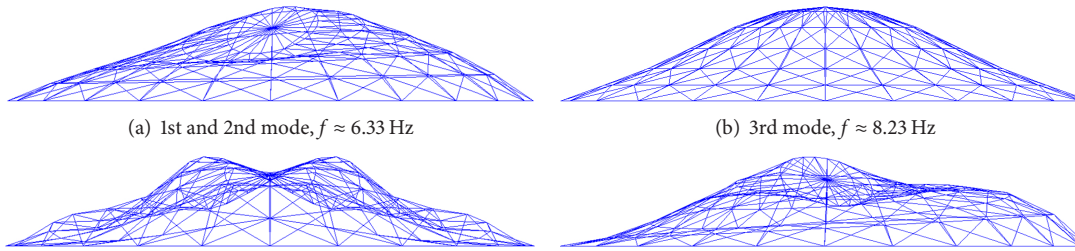

(a) 1st and 2nd mode, $f \approx 6.33$ Hz (b) 3rd mode, $f \approx 8.23$ Hz

(c) 4th and 5th mode, $f \approx 8.77$ Hz (d) 6th and 7th mode, $f \approx 8.89$ Hz

Figure 6: The mode shapes and corresponding frequencies of the Schwedler latticed shell.

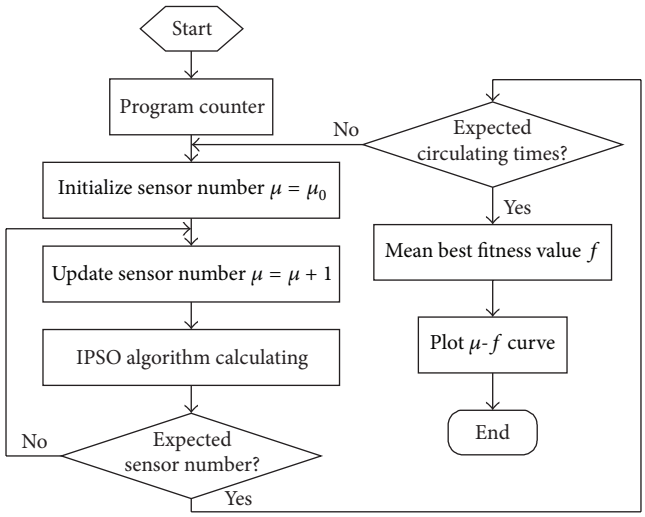

Figure 7: Flow chart of optimizing sensor number.

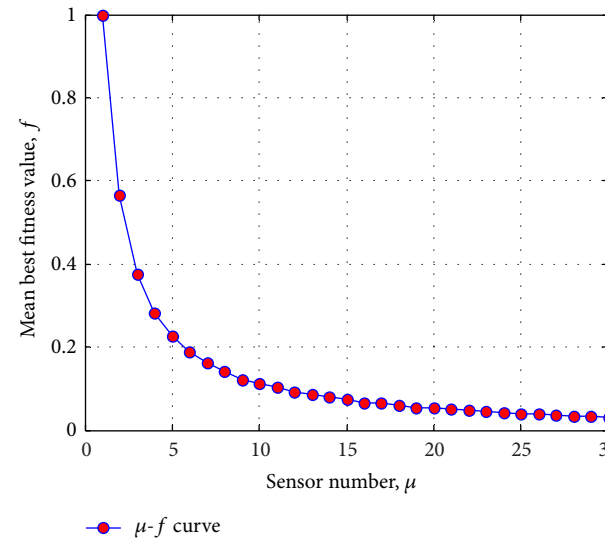

Figure 8: Relationship between the sensor number (μ) and the mean best fitness value (f).

in (20). The maximum number of allowable iterations, t_{max}, for the optimization algorithm is set to 4000 to ensure that the algorithms determine the optimal sensor placement and observe the variation of the fitness value with respect to the iterations. For a fair comparison, the other settings of the parameters are the same as mentioned above, including the mutation probability, acceleration coefficients, population size, and maximum velocity. The computation result of the EI method and the best fitness values of the five different PSO algorithms are listed in Table 4.

From the maximum off-diagonal elements (ODE_{max}) of the MAC matrix presented in Table 4, the five PSO optimization algorithms can clearly minimize the ODE_{max}. This result indicates that the PSO algorithms can be utilized to solve the OSP problem. The RMS values of the off-diagonal elements (ODE_{rms}) are all close to each other, but the proposed IPSO algorithm can obtain the minimum value. This result verifies the proposed algorithm's superiority. The conclusions can

Table 4: Maximum values (ODE_{max}) and root-mean-square values of off-diagonal elements (ODE_{rms}) of MAC matrix for 20 DOFs obtained by the six different methods.

Method	EI	SPSO	LPSO	RPSO	NPSO	IPSO
ODE_{max}	0.1663	0.1382	0.1330	0.1281	0.1096	0.0963
ODE_{rms}	0.0377	0.0368	0.0415	0.0378	0.0328	0.0321

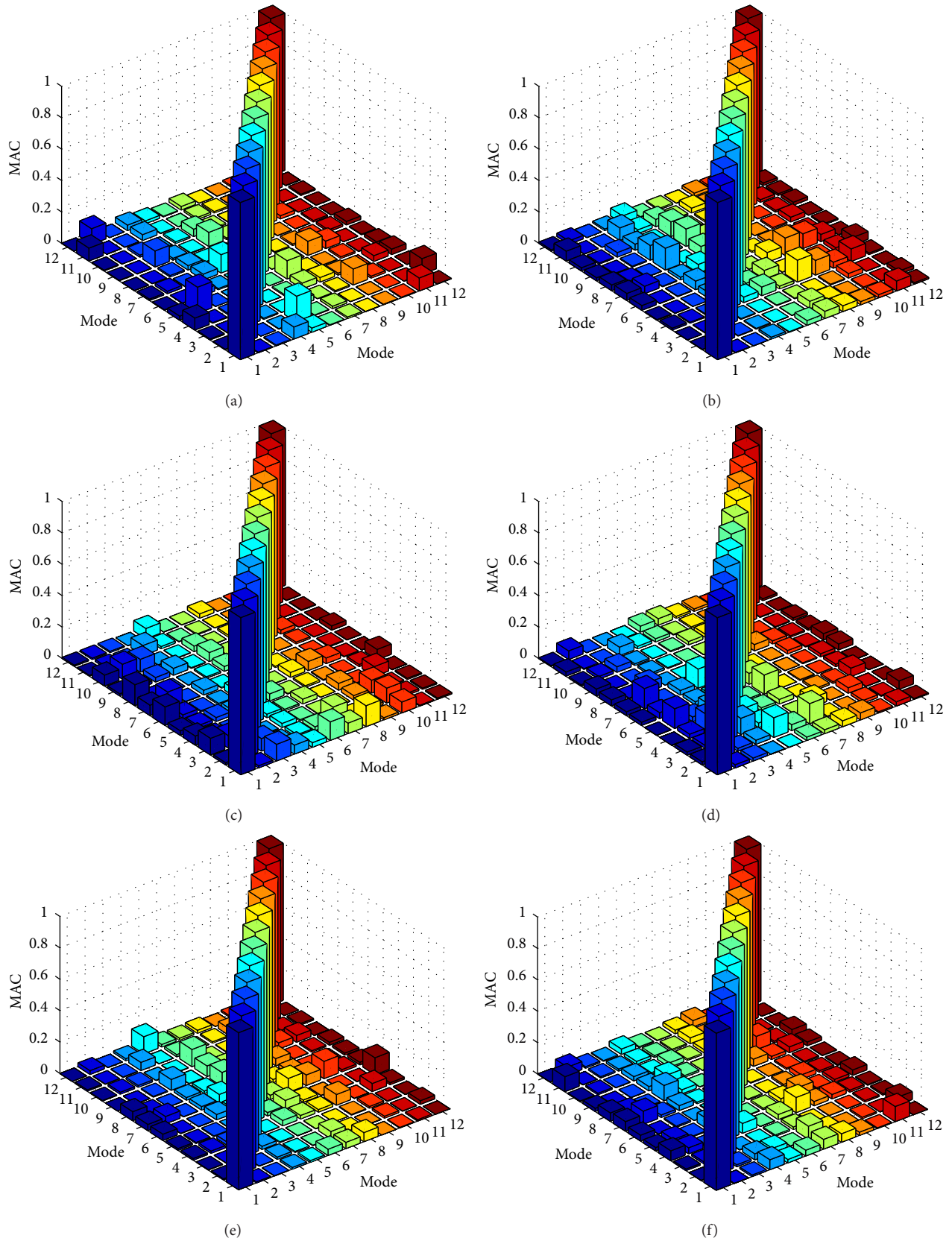

Figure 9: MAC values of 20 DOFs obtained by the six different methods. (a) EI method. (b) SPSO method. (c) LPSO method. (d) RPSO method. (e) NPSO method. (f) IPSO method.

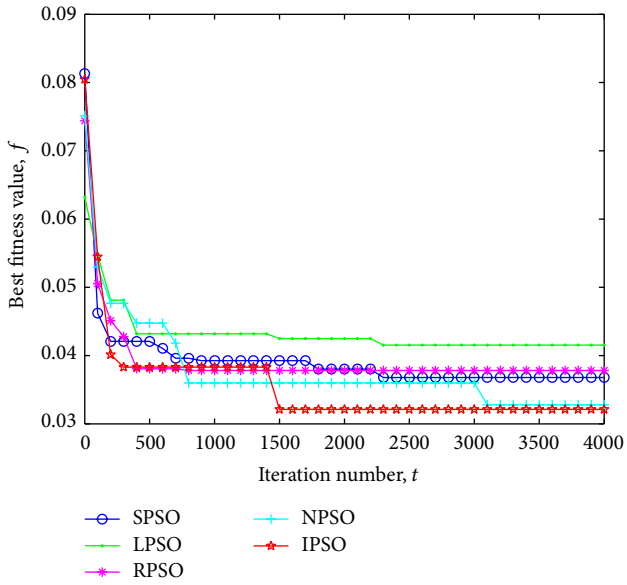

FIGURE 10: Performances of the five PSO algorithms.

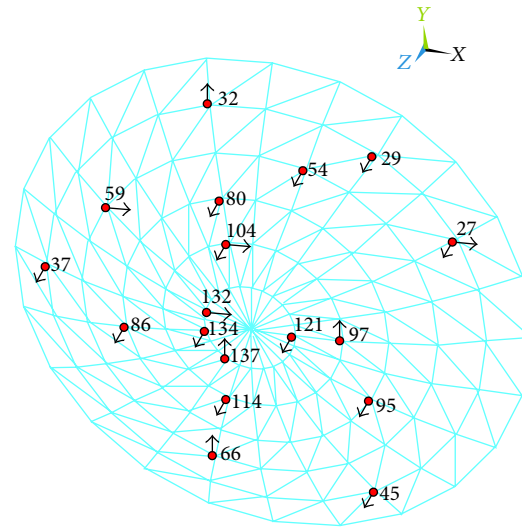

FIGURE 11: Optimal placement result of IPSO algorithm.

also be reached from the distribution of the MAC values from the six different methods given in Figure 9. All of the off-diagonal elements are intuitionally displayed in this figure. The proposed IPSO algorithm can obtain smaller values compared with the other five methods. In Figure 10, the best fitness values of the five PSO algorithms are compared. The IPSO algorithm can clearly determine the minimum fitness among these optimization algorithms. Finally, the placement results in three directions of the IPSO algorithm are given in Figure 11.

4.5. Discussion. The presentation case is based on the FEM of a latticed shell structure, which is created in strict accordance with the actual structure. Therefore, the validity of the proposed IPSO algorithm and the obtained optimal placement scheme can be verified by the comparison simulation results. However, this study still has some inevitable limitations. For example, the IPSO algorithm performance with different k values is not presented. Thus, the determination of k may be empirical to a certain extent. The FEM errors may also impact the placement results that are not considered in the simulation experiments. However, this problem could be solved if we consider a sensor placement experiment on a real latticed shell structure.

5. Conclusions and Future Work

In this paper, a novel IPSO approach is presented to address the existing defects of the traditional sensor placement methods. Firstly, a new method is proposed to select the mode number. Three strategies are then adopted to improve the PSO algorithm. Finally, the proposed IPSO approach is applied to determine the optimal sensor number and locations. With simulation experiments, some conclusions are summarized as follows.

(1) In selecting the proper modes, a new method called cumulative effective modal mass participation ratio is proposed, which can reflect the dynamic response of the given modes. Using this method, the sufficient main modes can be selected.

(2) Strategies such as the dual-structure coding, novel nonlinear inertia weight adjustment method, and mutation operator can be utilized to improve the PSO algorithm's search ability.

(3) The optimal sensor number is determined by a circulating computation strategy. This method calculates the mean best fitness value with the increase in sensor number. Therefore, the computation result is precise and reliable.

(4) The contrast simulation results with the EI method and four different PSO algorithms for a latticed shell structure show that the proposed IPSO algorithm has better enhancement in convergence speed and precision.

The effectiveness of the IPSO approach has been proven in this study through simulation experiments. However, some aspects need to be further studied. The model errors should be investigated in future research.

Conflict of Interests

The authors declare that there is no conflict of interests regarding the publication of this paper.

References

[1] D. S. Shan, Z. H. Wan, and L. Qiao, "Optimal sensor placement for long-span railway steel truss cable-stayed bridge," in *Proceedings of the 3rd International Conference on Measuring Technology and Mechatronics Automation (ICMTMA '11)*, pp. 795–798, January 2011.

[2] D. C. Kammer, "Sensor placement for on-orbit modal identification and correlation of large space structures," *Journal of Guidance, Control, and Dynamics*, vol. 14, no. 2, pp. 251–259, 1991.

[3] F. E. Udwadia, "Methodology for optimum sensor locations for parameter identification in dynamic systems," *Journal of Engineering Mechanics*, vol. 120, no. 2, pp. 368–390, 1994.

[4] D. C. Kammer and M. L. Tinker, "Optimal placement of triaxial accelerometers for modal vibration tests," *Mechanical Systems and Signal Processing*, vol. 18, no. 1, pp. 29–41, 2004.

[5] M. Meo and G. Zumpano, "On the optimal sensor placement techniques for a bridge structure," *Engineering Structures*, vol. 27, no. 10, pp. 1488–1497, 2005.

[6] C. Papadimitriou, "Optimal sensor placement methodology for parametric identification of structural systems," *Journal of Sound and Vibration*, vol. 278, no. 4-5, pp. 923–947, 2004.

[7] C. Papadimitriou, "Pareto optimal sensor locations for structural identification," *Computer Methods in Applied Mechanics and Engineering*, vol. 194, no. 12–16, pp. 1655–1673, 2005.

[8] I. Trendafilova, W. Heylen, and H. Van Brussel, "Measurement point selection in damage detection using the mutual information concept," *Smart Materials and Structures*, vol. 10, no. 3, pp. 528–533, 2001.

[9] C. Schedlinski and M. Link, "An approach to optimal pick-up and exciter placement," *Proceeding of SPIE International Society for Optical Engineering*, pp. 376–382, 1996.

[10] Y. S. Park and H. B. Kim, "Sensor placement guide for model comparison and improvement," *Proceeding of SPIE International Society For Optical Engineering*, pp. 404–409, 1996.

[11] A. P. Cherng, "Optimal sensor placement for modal parameter identification using signal subspace correlation techniques," *Mechanical Systems and Signal Processing*, vol. 17, no. 2, pp. 361–378, 2003.

[12] M. Reynier and H. Abou-Kandil, "Sensors location for updating problems," *Mechanical Systems and Signal Processing*, vol. 13, no. 2, pp. 297–314, 1999.

[13] J. E. T. Penny, M. I. Friswell, and S. D. Garvey, "Automatic choice of measurement locations for dynamic testing," *AIAA journal*, vol. 32, no. 2, pp. 407–414, 1994.

[14] C. B. Larson, D. C. Zimmerman, and E. L. Marek, "A comparison of modal test planning techniques: excitation and sensor placement using the NASA 8-bay truss," *Proceeding of SPIE International Society for Optical Engineering*, pp. 205–205, 1994.

[15] G. Heo, M. L. Wang, and D. Satpathi, "Optimal transducer placement for health monitoring of long span bridge," *Soil Dynamics and Earthquake Engineering*, vol. 16, no. 7-8, pp. 495–502, 1997.

[16] W. Heylen and P. Sas, *Modal Analysis Theory and Testing*, Departement Werktuigkunde, Katholieke Universteit Leuven, 2006.

[17] G. C. Marano, G. Monti, and G. Quaranta, "Comparison of different optimum criteria for sensor placement in lattice towers," *Structural Design of Tall and Special Buildings*, vol. 20, no. 8, pp. 1048–1056, 2011.

[18] L. Yao, W. A. Sethares, and D. C. Kammer, "Sensor placement for on-orbit modal identification via a genetic algorithm," *AIAA journal*, vol. 31, no. 10, pp. 1922–1928, 1993.

[19] R. R. Brooks, S. S. Iyengar, and J. Chen, "Automatic correlation and calibration of noisy sensor readings using elite genetic algorithms," *Artificial Intelligence*, vol. 84, no. 1-2, pp. 339–354, 1996.

[20] W. Liu, W. C. Gao, Y. Sun, and M. J. Xu, "Optimal sensor placement for spatial lattice structure based on genetic algorithms," *Journal of Sound and Vibration*, vol. 317, no. 1-2, pp. 175–189, 2008.

[21] G. Ma, F. L. Huang, and X. M. Wang, "Optimal placement of sensors in monitoring for bridge based on hybrid genetic algorithm," *Journal of Vibration Engineering*, vol. 21, no. 2, pp. 191–196, 2008.

[22] K. D. Dhuri and P. Seshu, "Multi-objective optimization of piezo actuator placement and sizing using genetic algorithm," *Journal of Sound and Vibration*, vol. 323, no. 3—5, pp. 495–514, 2009.

[23] Y. J. Cha, A. K. Agrawal, Y. Kim, and A. M. Raich, "Multi-objective genetic algorithms for cost-effective distributions of actuators and sensors in large structures," *Expert Systems with Applications*, vol. 39, no. 9, pp. 7822–7833, 2012.

[24] C. He, J. C. Xing, J. L. Li et al., "A combined optimal sensor placement strategy for the structural health monitoring of bridge structures," *International Journal of Distributed Sensor Networks*, vol. 2013, Article ID 820694, 9 pages, 2013.

[25] A. R. M. Rao and G. Anandakumar, "Optimal placement of sensors for structural system identification and health monitoring using a hybrid swarm intelligence technique," *Smart Materials and Structures*, vol. 16, no. 6, pp. 2658–2672, 2007.

[26] J. J. Lian, L. J. He, B. Ma et al., "Optimal sensor placement for large structures using the nearest neighbour index and a hybrid swarm intelligence algorithm," *Smart Materials and Structures*, vol. 22, no. 9, Article ID 095015, 2013.

[27] L. J. He, J. J. Lian, B. Ma, and H. J. Wang, "Optimal multiaxial sensor placement for modal identification of large structures," *Structural Control and Health Monitoring*, vol. 21, no. 1, pp. 61–79, 2014.

[28] R. C. Eberhart and J. Kennedy, "New optimizer using particle swarm theory," in *Proceedings of the 6th International Symposium on Micro Machine and Human Science*, pp. 39–43, October 1995.

[29] J. Kennedy and R. C. Eberhart, "Particle swarm optimization," in *Proceedings of the IEEE International Conference on Neural Networks*, pp. 1942–1948, December 1995.

[30] E. L. Wilson, *Three-Dimensional Static and Dynamic Analysis of Structures. Computers and Structures*, CSI, Berkeley, Calif, USA, 2002.

[31] T. H. Yi, H. N. Li, and M. Gu, "Optimal sensor placement for health monitoring of high-rise structure based on genetic algorithm," *Mathematical Problems in Engineering*, vol. 2011, Article ID 395101, 12 pages, 2011.

[32] Y. H. Shi and R. C. Eberhart, "A modified particle swarm optimizer," in *Proceedings of the IEEE International Conference on Evolutionary Computation*, pp. 69–73, May 1998.

[33] Y. H. Shi and R. C. Eberhart, "Empirical study of particle swarm optimization," in *Proceedings of the IEEE Congress on Evolutionary Computation*, pp. 1945–1950, 1999.

[34] R. C. Eberhart and Y. H. Shi, "Tracking and optimizing dynamic systems with particle swarms," in *Proceedings of the Congress on Evolutionary Computation*, pp. 94–100, May 2001.

[35] A. Chatterjee and P. Siarry, "Nonlinear inertia weight variation for dynamic adaptation in particle swarm optimization," *Computers and Operations Research*, vol. 33, no. 3, pp. 859–871, 2006.

[36] A. Ratnaweera, S. K. Halgamuge, and H. C. Watson, "Self-organizing hierarchical particle swarm optimizer with time-varying acceleration coefficients," *IEEE Transactions on Evolutionary Computation*, vol. 8, no. 3, pp. 240–255, 2004.

[37] T. G. Carne and C. R. Dohrmann, "A modal test design strategy for modal correlation," *Proceeding of SPIE International Society for Optical Engineering*, pp. 927–927, 1995.

[38] J. Teng and Y. H. Zhu, "Optimal sensor placement for modal parameters test of large span spatial steel structural," *Engineering Mechanics*, vol. 28, no. 3, pp. 150–156, 2011 (Chinese).

[39] P. Kohnke, *ANSYS Theory Manual*, ANSYS Inc, 2001.

[40] J. S. Zhang, Y. Wu, and S. Z. Shen, "Identification of natural modes with significant contributions to wind-induced vibration of single-layer reticulated shell," *Journal of Vibration Engineering*, vol. 19, no. 4, pp. 452–458, 2006 (Chinese).